

Received July 7, 2019, accepted July 29, 2019, date of publication August 5, 2019, date of current version September 18, 2019.

Digital Object Identifier 10.1109/ACCESS.2019.2933287

# sEMG-Based Detection of Compensation Caused by Fatigue During Rehabilitation Therapy: A Pilot Study

SHUANGYUAN HUANG<sup>1</sup>, SIQI CAI<sup>1</sup>, GUOFENG LI, YAN CHEN, KE MA, AND LONGHAN XIE

Shien-Ming Wu School of Intelligent Engineering, South China University of Technology, Guangzhou 510640, China

Corresponding author: Longhan Xie (melhxie@scut.edu.cn)

This work was supported in part by the National Natural Science Foundation of China under Grant 51575188, in part by the National Key Research and Development Program of China under Grant 2018YFB1306201, in part by the Research Foundation of Guangdong Province under Grant 2016A030313492 and Grant 2019A050505001, and in part by the Guangzhou Research Foundation under Grant 201903010028.

**ABSTRACT** To stimulate neuroplasticity, the stroke patient often receives repetitive and high load robotic rehabilitation therapy. Given their impaired motor function, the patients are prone to muscle fatigue. Muscle fatigue lead patients to compensate for upper limb motion by recruiting trunk and shoulder motions, resulting in undesirable rehabilitation motion and a subsequent risk of injury. However, fatigue compensation is not detected during upper-limb robotic rehabilitation training in the existing rehabilitation robot. The aim of this study was to detect the compensation caused by fatigue based on surface electromyography (sEMG). Eight healthy subjects performed three basic repetitive resistance rehabilitation training tasks, to elicit three types of common stroke fatigue compensatory synergies. The subjective fatigue score and sEMGs of the main muscles used were acquired to determine the fatigue state. The compensatory motion was recorded by a motion capture apparatus. The sEMG median frequency (MDF) of the main muscles used and the overall fatigue compensation were calculated. With the development of fatigue, the subjects exhibited more signs of fatigue compensation. The motion types slightly increased the degree of corresponding basic compensation. However, the subjects exhibited similar ranges and trends in the overall compensation. A strong correlation was found between sEMG MDF and overall fatigue compensation. Thus, fatigue compensation can be detected based on the body's status regardless of the type of motion. The sEMG-based detection of fatigue compensation proposed in this study is a reliable way to detect fatigue compensation and improve the quality of therapeutic exercise during upper-limb robotic rehabilitation training.

**INDEX TERMS** Rehabilitation, fatigue compensation, stroke, detection.

## I. INTRODUCTION

Stroke is the leading cause of acquired disability for adults [1]. Stroke, which is the result of a blood supply shortage to the brain or cerebral hemorrhage, leads to brain cell death and the disruption of the intricate internal circuits of the brain [2], [3]. Depending on the lesion locations, strokes may damage the motor and sensory neural system and frequently lead to permanent neurological impairment that is associated with serious physical and cognitive dysfunction [2], [3]. Because of the impairments, most stroke survivors lose the ability to perform daily activities [4], [5].

The associate editor coordinating the review of this manuscript and approving it for publication was Rajeeb Dey.

According to neuroplasticity, which describes how the human central nervous system can structurally and functionally adapt to acquire new skills, highly repetitive rehabilitation exercise can help recover physical and cognitive abilities [6], [7]. However, most stroke survivors do not benefit from therapeutic exercise because of the shortage of medical resources. Robotic stroke rehabilitation therapy, which has the potential to improve the recovery process for stroke survivors, can deliver highly intense repetitive training [8].

A major problem that degrades the quality of therapeutic exercise is undesired compensatory motion [9]. According to neuroplasticity, the end motion stimulates specific brain areas, and the compensatory motion cannot stimulate the subjects' brains appropriately. Such compensation hinders the

process of recovery and can introduce additional orthopedic problems [10]. The end-effector rehabilitation robots, including the MIT-MANUS [11], MIME [12] and GENTLE/s [13] robots, allow for many degrees of freedom at various joints. As a consequence, generating an isolated movement at a single upper limb joint is difficult since the movement of the end effector can cause a combination of movements at the wrist, elbow and shoulder joints [14]. If the exercise motions are difficult for the stroke survivors or if the survivors are fatigued, they tend to compensate for the upper limb motion by moving the trunk and shoulder. The stroke survivors' type of compensation during rehabilitation can be classified as either pathologic compensation or fatigue compensation. Pathologic compensation is caused by motor dysfunction because of injury to the central nervous system [15]. Fatigue compensation occurs due to muscle fatigue. The traditional way to reduce compensation is through hardware fixation, but fastening the patient's trunk to a chair is unsafe and uncomfortable [16]. Thus, many methods for detecting and reducing pathologic compensation have been proposed. Using the Kinect-tracked to automatically detect compensation has been proposed, which can detect the compensation of healthy subjects. However, the same classifiers performed poorly in detecting compensation in stroke survivors [17]. The games are used to encourage users to perform therapeutic exercises correctly by reducing the compensatory motions, and they currently require the supervision of a therapist [10]. The multimodal feedback regarding the stroke survivors' trunk compensation levels resulted in reduced trunk displacement. No difference between the feedback modalities was obtained. The positive effects of including the game scores might not have been observed in the 4 short-term interventions. Longer studies should investigate whether the use of game scores could result in trunk compensation improvements when compared to the trunk restraint strategies [18]. Regardless of vision, game scores or accelerometer are all based on the detection of the kinematic parameters, but the compensation in the organism is neglected. Although the kinematic parameters would be particularly suitable for assessing the movement quality during rehabilitation exercises, there is a lack of information on the coordination in the muscle degree.

Even if pathologic compensation is detected, it is difficult to reduce and eliminate it. Nevertheless, fatigue compensation, which is caused by motor fatigue during training, can be avoided through fatigue compensation detection and by controlling the training strategy. To obtain sufficient stimulation to the central nervous system, the rehabilitation training motions are generally repetitive and are sustained for approximately ten to twenty minutes in a single exercise session [19]. However, the repetitive nature of the training could cause motor fatigue, and then fatigue compensatory movement occurs. Fatigue compensation could limit the gains in motor function by learned nonuse and may lead to pain and joint contractures in the long term [20]. Nevertheless, compensation caused by fatigue was not detected by the rehabilitation robot.

The purpose of this article is to propose the detection of fatigue compensation during upper limb rehabilitation training. Fatigue compensatory movements in the shoulder, neck, and trunk of some patients have been observed in clinical studies and are caused by the highly repetitive rehabilitation training exercises [21]–[23]. The existence of muscle synergies or compensation in the production of movements is not restricted to pathology but may reflect a general principle of neural control [24], [25]. There were 8 patients and 6 healthy subjects performed seven motor tasks involving the shoulder and elbow joints. The muscle synergies or muscle compensation extracted from sEMG of patients and healthy subjects were very consistent across individuals [26]. The healthy subjects' sEMG features in the term of muscle synergies can be a good reference meaning for the stroke. Thus, healthy people were selected as the subjects to conduct this study. We proposed resistance training for the subjects during the upper limb rehabilitation exercises, including three basic motions: reaching up-and-down (UD), reaching side-to-side (SS), and reaching forward-and-back (FB), for approximately 220–240 seconds, to elicit the three basic fatigue compensatory movements: trunk-rotation, lean-forward and shoulder-elevation movements. The motion compensations were captured by the motion capture apparatus. The sEMG median frequency (MDF) and a subjective fatigue score were used to determine the development of muscular and mental fatigue. With the decrease of the sEMG MDF, fatigue compensation increases. There is a strong correlation between the sEMG MDF of the main muscles used and the level of fatigue compensation. The sEMG MDF of the main muscles used can reliably detect fatigue compensation, which is convenient and feasible in rehabilitation training.

## II. METHODS

### A. PARTICIPANTS

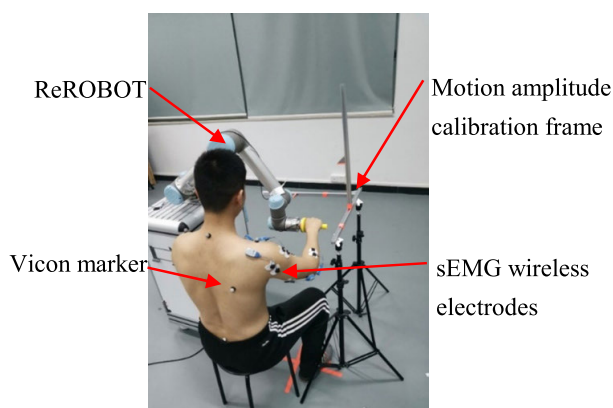
Eight healthy subjects were selected to participate in the experiment. They were 8 males, with no neurological, sensorimotor, or orthopedic impairments, as shown in Table 1. All of the subjects selected had no understanding of fatigue compensation. Prior to the experiment, a signed informed consent form was obtained from all the subjects.

### B. EXPERIMENTAL SETUP AND MEASUREMENT PROCEDURE

The data acquisition and rehabilitation training experiments were conducted on the ReROBOT platform, as shown in Figure 1, which was developed in our laboratory. The ReROBOT platform consists of the ReROBOT, Vicon (Oxford Metrics plc, Oxford), myoMUSCLE (NORAXON, Arizona), and motion amplitude calibration frame. The ReROBOT can provide several rehabilitation training modes. The subjects' shoulder and trunk motions could be accurately captured at 100 Hz with the 11 camera capture system. The raw sEMG signal was acquired at 2000 Hz by the myoMUSCLE. To make the motion amplitude uniform, there are motion

**TABLE 1.** Details of the eight subjects.

Subject	Gender	Age (years)	Height (cm)	Weight (kg)	Handedness
S1	M	28	168	69	Right
S2	M	22	181	62	Right
S3	M	25	170	60	Right
S4	M	22	169	56	Right
S5	M	30	172	67	Right
S6	M	23	171	65	Right
S7	M	23	180	75	Right
S8	M	26	164	68	Right

**FIGURE 1.** The ReROBOT platform.

amplitude markers attached at the motion amplitude calibration frame, which enable the subjects to know the motion amplitude during the training.

Because stroke patients easily reach a state of motor fatigue, to better approximate the patients' muscle fatigue state, a repeat resistance mode of exercise is chosen in this article. Resistance training has become common in rehabilitation. The stroke patients are mainly elderly and their muscle mass and muscle strength decreases by approximately 30% between the third and sixth decades of life [27]. Through adapted resistance exercises, it is possible to promote an increase in muscle mass and muscle strength, which is the base of functional recovery [28], [29]. The ReROBOT repeat resistance mode for rehabilitation constantly applies a resistance to the movements generated by the subject in all six degrees of freedom. The level of resistance can be adjusted in all six degrees of freedom according to the capabilities of the subject. The maximal resistance is calibrated based on a healthy male with an average height and weight perception when the ReROBOT negates almost all the patient-generated movements in the associated degree of freedom.

The subjects repeatedly performed the three basic motion sessions, defined as reaching up-and-down (UD), reaching side-to-side (SS), and reaching forward-and-back (FB), at a

comfortable range and pace. The details of the motions are shown in Table 2. The motions were intended to elicit three types of common poststroke compensatory synergies: shoulder-elevation, trunk-rotation, and lean-forward [17], as shown in Table 2 and Figure 2.

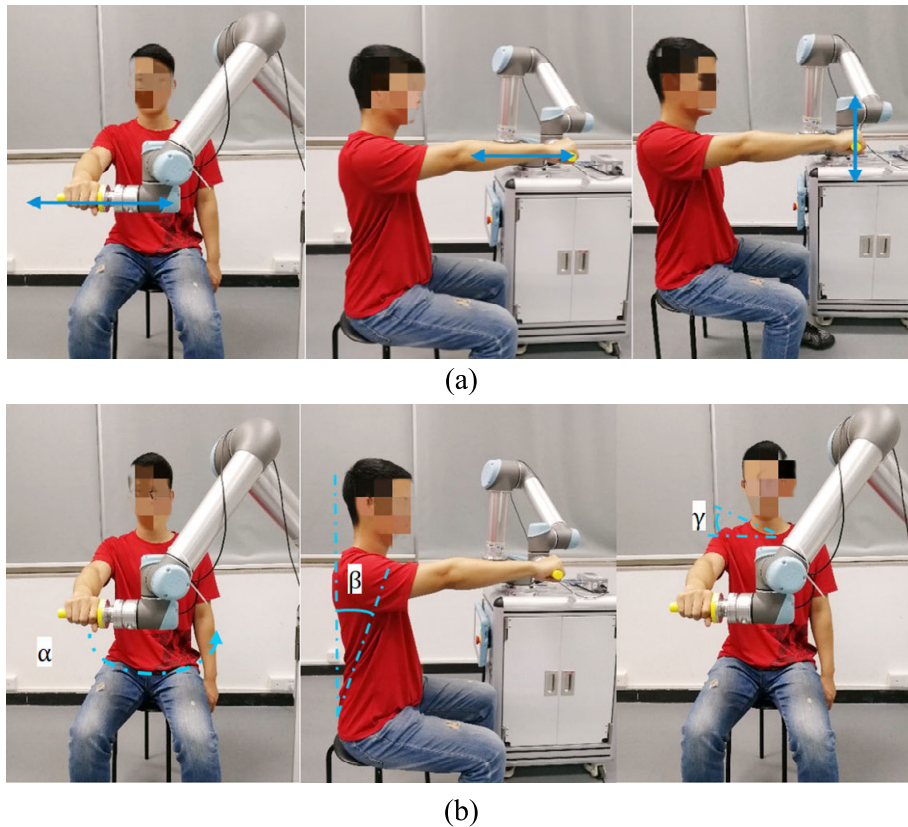
Prior to participation, the subjects were asked to place themselves in front of the ReROBOT; the subjects were given an explanation on how to use the device and a brief description of the motions to perform. To calibrate their motion amplitude, the subjects were required to perform the motions three times, and the end points of the motion amplitude marker were adjusted. During the training session, the subjects were required to attempt to keep the motion reaching range at the start and end motion amplitude marker. During the training sessions, the subjects were required to subjectively maintain the motion at the same speed, range, and trajectory. The subjects repeated each motion for approximately 220-240 seconds per task session, with 15 minutes of rest between the intervals. If a subject still felt fatigued at the end of the rest period, the rest time was increased until the subject felt absolutely relaxed.

The shoulder and trunk motions were tracked with the VICON using 5 reflective markers attached to the right shoulder acromio-clavicular joint, left shoulder acromio-clavicular joint, spinous process of the 7<sup>th</sup> cervical vertebra, spinous process of the 10<sup>th</sup> thoracic vertebra, and right scapula. The shoulder elevation was tracked using markers placed bilaterally on the right shoulder acromio-clavicular joint, left shoulder acromio-clavicular joint and spinous process of the 7<sup>th</sup> cervical vertebra. The trunk rotation was tracked using markers on the right shoulder acromio-clavicular joint and spinous process of the 7<sup>th</sup> cervical vertebra. The lean-forward motion was tracked using the spinous process of the 7<sup>th</sup> cervical vertebra and spinous process of the 10<sup>th</sup> thoracic vertebra. A reference marker was placed on the right scapula.

Six sEMG wireless electrodes were attached to the main muscles of the right arm, including the anterior, middle, and posterior deltoids and the triceps, biceps, and brachioradialis. Because the sEMG voltages are very low in magnitude

**TABLE 2.** Description of movement tasks and compensations.

Motion	Basic compensatory type	Description	Resistance force level
Reaching side-to-side (SS)	Trunk-rotation(Tr), $\alpha$ .	Move the handle from side to side in a straight trajectory that is parallel to the frontal axis on the transverse plane.	25%
Reaching forward-and-back (FB)	Lean-forward (Lf), $\beta$	Move the handle back and forth in a straight trajectory that is parallel to the sagittal axis on the transverse plane.	35%
Reaching up-and-down (UD)	Shoulder-elevation (Se), $\gamma$ .	Move the handle up and down in a straight trajectory that is parallel to the vertical or longitudinal axis on the sagittal plane.	20%

**FIGURE 2.** The three basic motion and compensation types: (a) Three basic motion types: SS, FB, and UD. (b) Three basic compensation types: TR, LR, SE.

(0-5 mV) and have considerable noise content, the original analog signal must be amplified. In this study, the raw sEMG signals were amplified by a factor of 1000 times. Because the information content of an sEMG signal usually lies in the 20 to 500 Hz frequency domain, the raw sEMG signals were sampled at 2 kHz according to the Nyquist theorem [30].

To rate their subjective upper limb fatigue, the subjects assessed themselves according to the rating of perceived exertion scale (RPE) [31], as shown in Table 3, in each 30 second time period during the training session. The subjects were asked: “How tired does your arm feel at the moment?” and they had to reply with a fatigue score. All subjects performed three types of reaching motions with their dominant hand.

### III. DATA ANALYSIS

#### A. DATA PROCESS

Three outcome measures were collected in the experiment: the sEMG median frequency, subjective fatigue score, and motion compensation.

The sEMG characteristics indicated the muscle state. Generally, muscle fatigue is shown by several sEMG indexes, including a decrease in the signal power at high frequency and an increase at low frequency, and also a decrease in the spectrum slope at high frequency and an increase at low frequency [33], [34]. In this article, the sEMG median frequency, which has been used as the gold standard for measuring muscle fatigue, was used to obtain the muscle

**TABLE 3.** Rating of perceived exertion scale [32].

Score	Descriptor
0	Rest
1	Very, very easy
2	Easy
3	Moderate
4	Somewhat hard
5	Hard
6	
7	Very Hard
8	
9	
10	Maximal

fatigue state. With muscle fatigue, the sEMG median frequency, which is less affected by random noise in the high frequency band of the sEMG power spectrum, is decreased in the frequency spectrum [35].

The raw sEMG signals were first bandpass filtered with cut-off frequencies of 10 Hz and 500 Hz and notch filtered at 50 Hz to reduce the noise content, as recommended by the European SENIAM project [36]. We used an overlap analysis window with a window length of 512 ms and a window sliding step size of 256 ms. Because the training was repetitive, the MDF during the active state could reflect the real muscle fatigue state [37]. Thus, the sEMG signal data were segmented to focus the analysis on the active segments. The root mean square (RMS) is directly related to the energy of the sEMG signal and can reflect the energy produced by the muscle to reflect the muscle activation status.

The RMS of the sEMG is calculated according to the following formula:

$$RMS(t) = \sqrt{\frac{1}{M} \sum_{k=1}^M sEMG^t(k)^2} \quad (1)$$

where  $t$  is the sequence number of windows,  $k$  is sEMG data in the  $t^{\text{th}}$  analysis window, and  $M$  is the total number of data points in the  $t^{\text{th}}$  window ( $M = 512$ ).

Then, the active segment is detected using a fixed threshold. The state function,  $s(l)$ , of the  $l^{\text{th}}$  analysis window is calculated as follows:

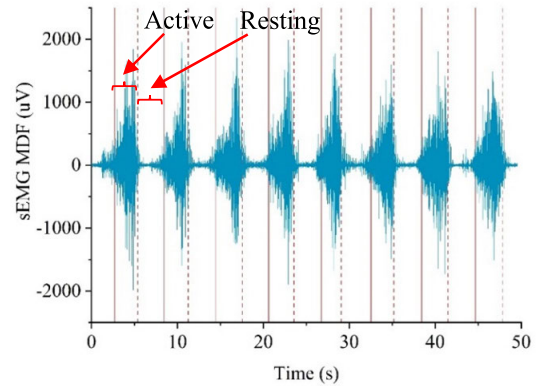
$$s(t) = \begin{cases} 0, & RMS(t) < Th \\ 1, & RMS(t) \geq Th \end{cases} \quad (2)$$

$$Th = 0.8 \frac{1}{n} \sum_{t=1}^k RMS(t) \quad (3)$$

where  $n$  is the total number of the current 20% task time windows. To avoid misclassification, the condition of the active segment based on the state function is:

$$\begin{cases} s(t_1 - 1) = 0 \text{ and } s(t_1) = 1 \\ s(t_2 - 1) = 1 \text{ and } s(t_2) = 0 \\ t_2 - t_1 \geq 3 * wlen \end{cases} \quad (4)$$

where  $t_1$  is the starting point of the active segment,  $t_2$  is the end point and  $wlen$  is the window length ( $wlen = 512$  ms).

**FIGURE 3.** Example of sEMG signal segmentation.

According to the duration of the motion, three window lengths are selected as the time threshold. An example of sEMG signal segmentation is shown in Figure 3.

The MDF indicates that the total power that is less than the median frequency is equal to the total power that is greater than the median frequency:

$$\int_0^{f_p} P(f) df = \frac{1}{2} \int_0^{f_s} /2P(f) df \quad (5)$$

$$MDF = f_p \quad (6)$$

where  $f_s$  is the sampling frequency ( $f_s = 2000$  Hz) and  $P(f)$  is the power spectral density of the signal.

Because of the differences in the subcutaneous tissue layers among the subjects and among the muscles of the same subject, the sEMG MDF is normalized by the initial median frequency.

$$normMDF = \frac{MDF}{MDF_{init}} \times 100\% \quad (7)$$

where  $MDF_{init}$  is the average MDF of the first 20% of the task time. The MDF are reported as a percentage of the initial normMDF.

The three basic motion compensations are presented by three angles, shown in Table 2 and Figure 2. The motion compensations are reported as the average compensation of every 20% of the task time relative to the average compensation of the first 20% of the task time. The overall compensation, which represents the holistic degree of compensation, is calculated by the sum of the three basic motion compensation angles:

$$\theta = \alpha + \beta + \gamma \quad (8)$$

where  $\alpha$ ,  $\beta$ , and  $\gamma$  represent the basic compensations, as shown in Table 2 and Figure 2.

The subject's motion range is kept constant by the motion amplitude calibration frame throughout the training session. The motion speed change can be represented by the change of motion repetitions, which can be acquired base on sEMG segment by equation (1)-(3).

$$normSpeed = \frac{h}{h_{init}} \times 100\% \quad (9)$$

TABLE 4. The meaning of R value.

R	Meaning
$0.0 \leq  R  < 0.2$	Very weak correlation or no correlation
$0.2 \leq  R  < 0.4$	Weak correlation
$0.4 \leq  R  < 0.6$	Moderate correlation
$0.6 \leq  R  < 0.8$	Strong correlation
$0.8 \leq  R  \leq 1.0$	Highly correlation

where  $h$  is the motion repetitions in each 20% task time,  $h_{init}$  is motion repetitions of the first 20% of the task time.

**B. STATISTICAL ANALYSIS**

All statistical analyses were performed using Matlab 2016b (MathWorks Inc. Natick, MA, USA). A Pearson correlation test was employed to estimate the linear correlation between sEMG MDF and the overall fatigue compensation, and the correlation between three sessions overall compensation.

The Pearson correlation coefficient, represented by  $R$  in this paper, is measured on a scale with no units and can take a value from  $-1$  through  $0$  to  $+1$ . If the sign of the correlation coefficient was positive, then a positive correlation would have existed. If the sign of the correlation coefficient was negative, then a negative correlation would have existed. The meaning of  $R$  value is shown in TABLE 4. The significance level was set at  $p = 0.05$  for all tests.

**IV. RESULTS AND DISCUSSION**

**A. RESULTS**

As expected, the training would increase the subjects' fatigue, which increased the subjective fatigue scores and the sEMG

MDF, and the motion compensations increased with the level of fatigue.

The subjective fatigue assessment can reflect the muscular and mental fatigue. Figure 4 gives an overview of the subjects' subjective fatigue scores over the three training sessions. As the exercise progressed, the subjects' fatigue gradually increased. The repetitive training tasks not only fatigued the subjects' muscles but also made them mentally fatigued. Comparing the results of each subject, the largest perception of fatigue is present in the UD session, the SS session is second, and the FB session is the smallest. However, the resistance force in the UD session was the smallest. In the UD session, the subject should offset the gravity of the arm, and the main muscles used, the anterior and middle deltoid, are weaker than in the other two sessions. For the three sessions, we observed a similar increasing trend and range of subjective fatigue scores. This is due to the differences in strength and subjective feelings of fatigue for each subject. During the rehabilitation training, the rehabilitation doctor can estimate the change in patient fatigue according to the change of score. However, it is difficult to reflect the patient's real fatigue level with the subjective fatigue score because of the different athletic abilities and subjective fatigue feelings. Specifically, if the patient's language and cognitive abilities are impaired, it is difficult for them to properly express their actual fatigue state. Thus, a more objective indicator is needed to demonstrate the patient's fatigue level.

According to the main muscles used in the three sessions, the triceps, biceps, and middle deltoid sEMG MDFs were selected as the compensation indicators of SS, FB, and UD, respectively. The sEMG MDF development is shown in Figure 5. The sEMG MDFs of the subjects decrease as the training progresses, except the S8 deltoid sEMG MDF during the FB session. Because the FB was a compound action,

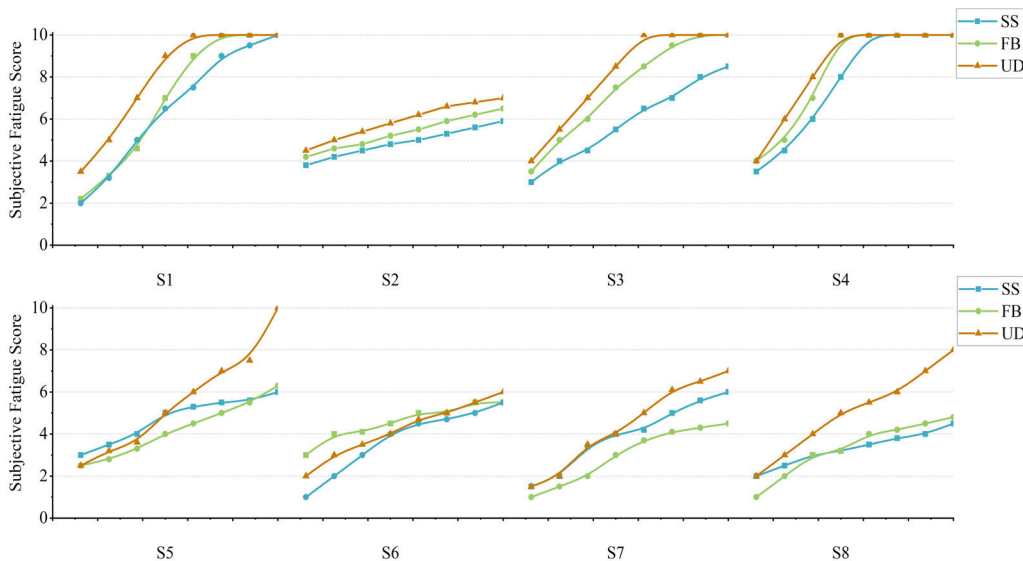
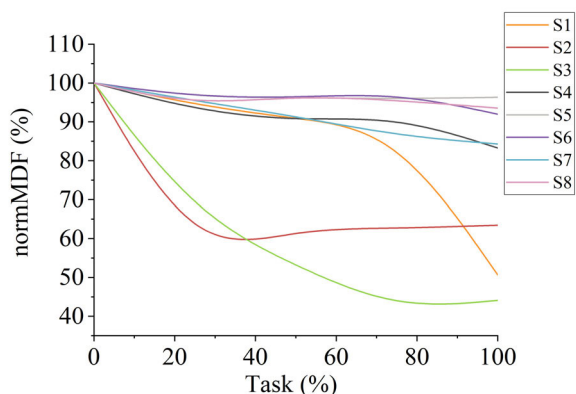
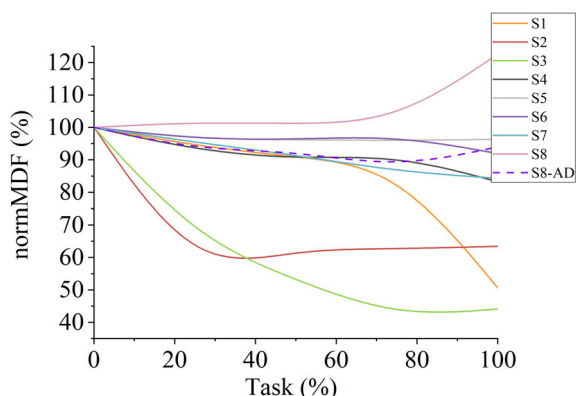


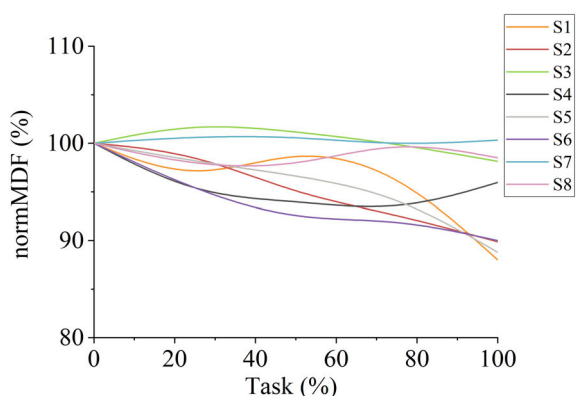
FIGURE 4. The subjective fatigue score during the 3 training sessions.



(a)



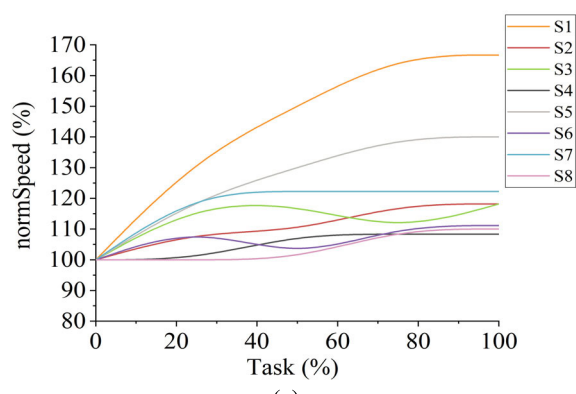
(b)



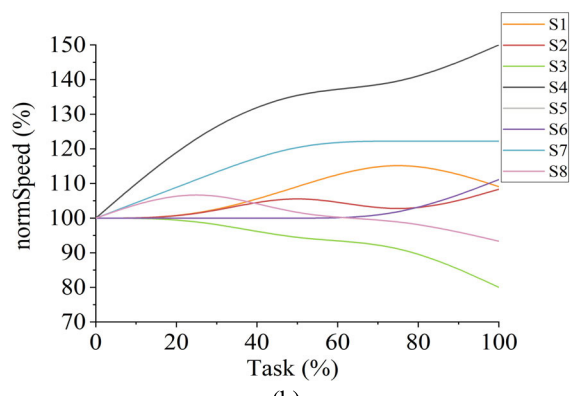
(c)

**FIGURE 5.** The MDF changes during 3 training sessions: (a) SS, (b) FB, and (c) UD.

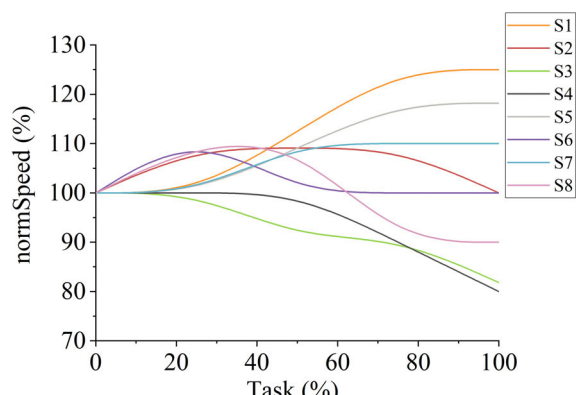
the S8 used anterior deltoid as agonist instead of middle deltoid. As shown in dashed line S8-AD of Figure 5 (b), the anterior deltoid sEMG MDF decreased in the FB session. Meanwhile, S8 decreased the movement velocity to relieve muscle fatigue, shown in Figure 6 (b). Thus, the S8 middle deltoid sEMG MDF increased in the FB session. The remaining MDF values did not decrease monotonically. Although the subjects were required to maintain the same pace throughout the training session, as the fatigue increased, the subjects unconsciously changed the movement velocity to relieve the fatigue, shown in Figure 6. The average R between the sEMG MDF and the velocity change is equal to  $-0.51$  means that



(a)



(b)



(c)

**FIGURE 6.** The velocity changes during the 3 training sessions: (a) SS, (b) FB, and (c) UD.

the sEMG MDF would increase with the movement velocity decrease. Moreover, the actions were compounded, and the subjects could compensate for the fatigued muscle by using other muscles. The compensation would change the subject's kinematic strategies, which were embodied in the increased compensation, making it difficult to maintain a consistent motion. Comparing the performance of the same subject in different training sessions, the sEMG MDF changed in a similar way. A similar method was used because of the athletic ability and the response strategy for fatigue.

The overall fatigue compensation is presented in Figure 7 (a), (c) and (e). During each session, fatigue compensation increased as the sEMG MDF decreased except

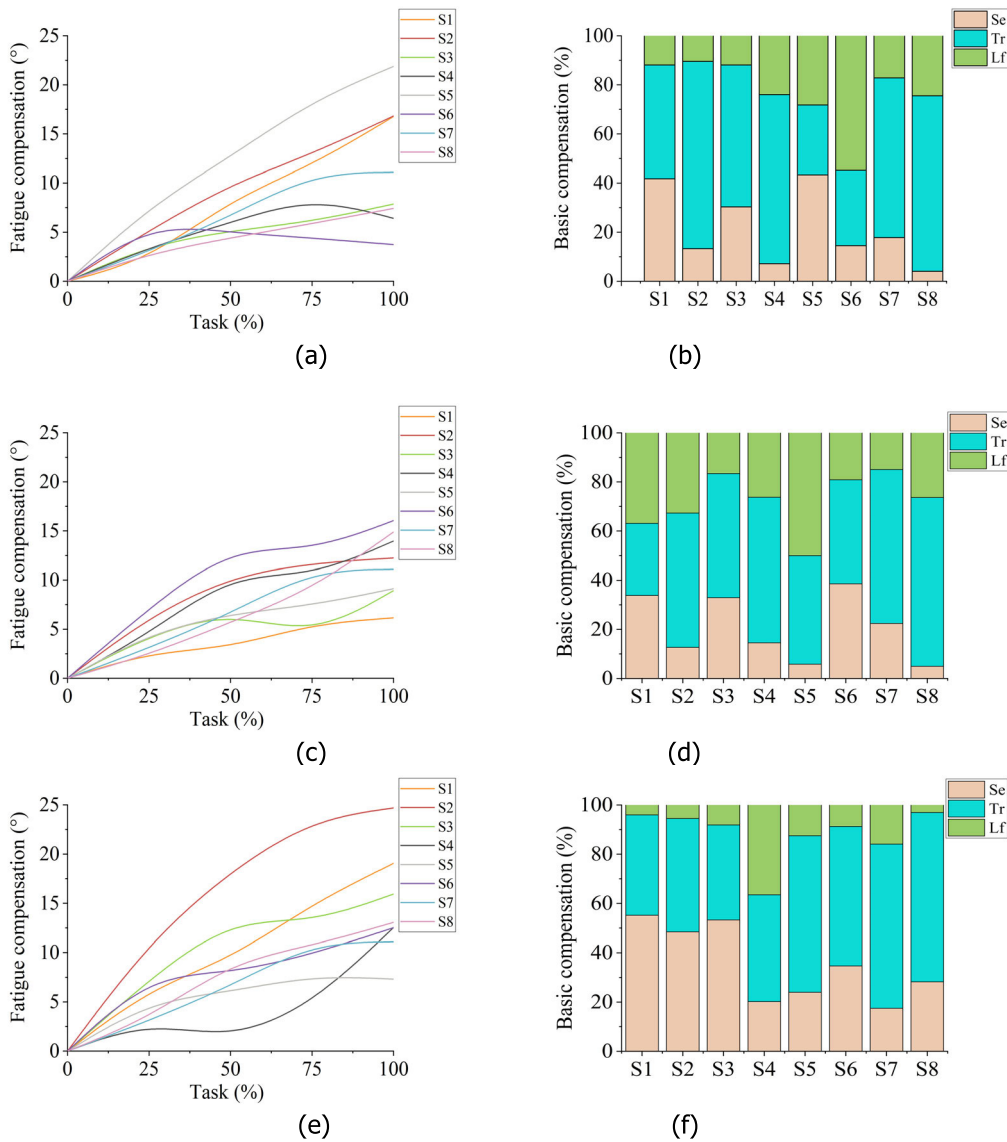


**FIGURE 7. Subject's overall fatigue compensation: (a) SS, (c) FB, (e) UD. The percentage of basic fatigue compensation: (b) SS, (d) FB, (f) UD.**

S8 during FB session. We noticed a similar increasing trend and range of the overall fatigue compensation for S1-S8 in different sessions, which is due to the characteristics of the athletic ability and strategy of the subject; For the S1-S8, the correlation of overall compensation in three sessions are shown in Table 5. Thus, the overall compensation caused by fatigue is independent of the motion type, which is different from pathologic compensation. This difference informed us that the detection of fatigue compensation should focus on the physical status but not the motion type. The percentages of the three basic compensations are illustrated in Figure 7 (b), (d) and (f). For the basic compensation, the largest TR percentage occurs in the SS session; the largest LF percentage occurs in the FB session, and the largest Se percentage occurs in the UD session. The average difference of Tr, Lf, Se, in the three sessions, are 15.3%, 13.3%,

15.8%, respectively. The high correlation between the overall compensation and little difference in the basic compensation indicates that fatigue compensation can be detected based on the fatigue status, regardless of the motion type.

In order to better describe the relationship between the fatigue compensation and sEMG MDF. With the high linear correlation between the sEMG MDF and fatigue, shown in Table 6, the average  $R = -0.848$  means the highly linear correlation, the linear regression was adopted:

$$CM = -0.186 - 78.21MD \quad (10)$$

With Goodness of fit  $R^2 = 0.9267$ . Where CM is the average of overall fatigue compensation. MD is the average of norm-MDF.

Some papers point out that fatigue can be better fitted by multivariable indexes [38]. Using this method as a reference,



**TABLE 5.** Correlation of overall compensation in three sessions ( $p < 0.05$ ).

	R ss, fb	R ss, ud	R ud, fb
S1	0.942	0.976	0.990
S2	0.957	0.977	0.994
S3	0.913	0.980	0.922
S4	0.884	0.512	0.733
S5	0.976	0.933	0.970
S6	0.644	0.720	0.945
S7	0.798	0.758	0.986
S8	0.958	0.983	0.946

Rss,fb = R of SS session and FB session, Rss,ud = R session of SS and UD session, Rud,fb = R of UD session and FB session.

**TABLE 6.** Correlation between the sEMG MDF and the overall compensation ( $p < 0.05$ ).

	SS	FB	UD
S1	-0.861	-0.679	-0.658
S2	-0.641	-0.943	-0.908
S3	-0.960	-0.7133	-0.939
S4	-0.730	<u>-0.151</u>	-0.940
S5	-0.798	-0.956	<u>0.160</u>
S6	<u>-0.487</u>	-0.692	-0.838
S7	-0.778	-0.890	-0.807
S8	-0.780	<u>0.834</u>	-0.961

we fitted average fatigue compensation through the average changes in velocity and sEMG MDF:

$$CM = -0.225 + 3.77SP - 74.93MD \quad (11)$$

With Goodness of fit  $R^2 = 0.9270$ . Where SP is the average of the normSpeed.

The performance of two approaches was highly similar. Because the effect of velocity change on fatigue compensation was implied by the influence of MDF change.

Based on the above analysis, we proposed detecting fatigue compensation based on the sEMG MDF regardless of the motion type, which is different from detecting pathological compensation. Only selecting the main muscles used can reliably detect fatigue compensation, which is convenient for rehabilitation training. Regardless of muscle or subjective fatigue, the subjects unconsciously engage in active muscular and motion compensation to protect the fatigued muscle when attempting to perform a normal motion. To acquire the optimal rehabilitation effect, it is important to consider the subject fatigue during the rehabilitation human-machine interaction. Based on the sEMG MDF of the active muscle, the subjects' fatigue compensation status can be detected. During the rehabilitation human-machine interaction, the sEMG MDF can be as the feedback of the fatigue compensation status, and

based on the detection, the rehabilitation robot can change the rehabilitation techniques and training strategies to improve the quality of the therapeutic exercise.

## B. DISCUSSION

In this paper, we studied the detection of fatigue compensation, which degrades the quality of therapeutic exercise during robotic upper limb stroke rehabilitation therapy. The overall compensation caused by fatigue is different from pathological compensation and can be detected regardless of the motion type. A significant correlation was found between fatigue compensation and the sEMG MDF of the main muscle used. Therefore, fatigue compensation detection based on the fatigue status is proposed in this article. Fatigue compensation can be well detected by the sEMG MDF from one or two of the major muscles used, which is convenient and feasible.

Research on fatigue compensatory behavior based on healthy subjects is also suitable for understanding stroke patients. It has been presented in a previous article that impaired motor function will exacerbate the extent of fatigue compensation. For instance, repetitive training would make the stroke survivor motor function decrease because the central nervous system is vulnerable to internal errors after a stroke so that it is likely to manifest as increases in sensorimotor noise over several motor repetitions [39]. Moreover, the compensatory motion observed in stroke patients may be increased by the reduced corticospinal drive, which compromises the ability of the nervous system to recruit spinal locomotor muscle synergies in the paretic limb [15].

It is considered important to ensure sufficient and repetitive rehabilitation training to stimulate neuroplasticity [34]. Unfortunately, tedious and repetitive training could fatigue patients who would then perform compensatory motions. Furthermore, the level of fatigue compensation could be aggravated, according to the extent of the neural deficits of the patients. In particular, early period of stroke, a patient easily becomes fatigued, and some patients develop strong and efficient motor compensation that prevents them from attempting to generate more normal motor patterns in their daily activities that may ultimately limit the final functional outcome [40]. In this case, rehabilitation is necessary to ensure the proper amount of exercise to stimulate the target neural pathways. However, during robotic rehabilitation training, the determination of the amount of training is often based on the subjective perception of the doctor, which may not be suitable for patients. Due to language and cognitive impairments and the difference in fatigue perceptions, it is difficult for patients to properly express the real fatigue state. The detection of fatigue compensation based on the sEMG MDF, which reflects the body's state during training, can be introduced as the feedback for the patient's fatigue compensation. It is useful to integrate adaptivity into robot-assisted upper limb rehabilitation based on the detected muscle fatigue experienced. In addition, the rehabilitation tasks should be diversified to prevent the patients from performing fatigue compensation movements.

Compared to the other compensation detection methods for pathological compensation, such as vision-based motion detection [17], [41], [42] and accelerometer detection assessment [43], the sEMG MDF detection for fatigue compensation can reflect the body's state. To our knowledge, there have been almost no studies that have investigated the detection of fatigue compensation. In the future, we will implement a fatigue compensation experiment on stroke patients. For the survivors, fatigue compensation would superpose pathological compensation and we could determine how to detect both kinds of compensation based on the sEMG. In addition, the patients' responses are diversified, and we should extract more features to reflect additional details of the compensation. For instance, fatigue compensation may be accompanied by tremors, which could also be detected by the sEMG.

## V. CONCLUSION

The sEMG-based detection of fatigue compensation proposed in this study proved to be a reliable and easy method for rehabilitation training. This work can be introduced to detect fatigue compensation in robotic rehabilitation therapy to avoid the risks of fatigue compensation and improve the quality of therapeutic exercise.

## REFERENCES

- [1] J. K. Burton, E. E. C. Ferguson, A. J. Barugh, K. E. Walesby, A. M. J. MacLulich, S. D. Shenkin, and T. J. Quinn, "Predicting discharge to institutional long-term care after stroke: A systematic review and meta-analysis," *J. Amer. Geriatrics Soc.*, vol. 66, no. 1, pp. 161–169, 2017.
- [2] T. Wieloch and K. Nikolich, "Mechanisms of neural plasticity following brain injury," *Current Opinion Neurobiol.*, vol. 16, no. 3, pp. 258–264, 2006.
- [3] W.-P. Teo and E. Chew, "Is motor-imagery brain-computer interface feasible in stroke rehabilitation?" *PM&R*, vol. 6, no. 8, pp. 723–728, 2014.
- [4] Y. John and F. Anne, "Review of stroke rehabilitation," *BMJ*, vol. 334, no. 7584, pp. 86–90, 2007.
- [5] R. L. Harvey, "Motor recovery after stroke: New directions in scientific inquiry," *Phys. Med. Rehabil. Clinics North Amer.*, vol. 14, no. 1, pp. S1–S5, 2003.
- [6] B. B. Johansson, "Current trends in stroke rehabilitation. A review with focus on brain plasticity," *Acta Neurologica Scandinavica*, vol. 123, no. 3, pp. 147–159, 2011.
- [7] A. Pascual-Leone, C. Freitas, L. Oberman, J. C. Horvath, M. Halko, M. Eldaief, S. Bashir, M. Vernet, M. Shafi, B. Westover, A. M. Vahabzadeh-Hagh, and A. Rotenberg, "Characterizing brain cortical plasticity and network dynamics across the age-span in health and disease with TMS-EEG and TMS-fMRI," *Brain Topography*, vol. 24, nos. 3–4, pp. 302–315, 2011.
- [8] E. D. Oña, R. Cano de la Cuerda, and P. Sánchez-Herrera, C. Balaguer, and A. Jardón, "A review of robotics in neurorehabilitation: Towards an automated process for upper limb," *J. Healthcare Eng.*, vol. 2018, pp. 1–19, 2018, Art. no. 9758939.
- [9] M. C. Cirstea and M. F. Levin, "Compensatory strategies for reaching in stroke," *Brain J. Neurol.*, vol. 123, no. 5, p. 940, 2000.
- [10] G. Alankus and C. Kelleher, "Reducing compensatory motions in video games for stroke rehabilitation," in *Proc. SIGCHI Conf. Hum. Factors Comput. Syst.*, 2012, pp. 2049–2058.
- [11] H. I. Krebs, J. J. Palazzolo, L. Dipietro, M. Ferraro, J. Krol, K. Ranekleiv, B. T. Volpe, and N. Hogan, "Rehabilitation robotics: Performance-based progressive robot-assisted therapy," *Autonom. Robot.*, vol. 15, no. 1, pp. 7–20, Jul. 2003.
- [12] C. G. Burgar, P. S. Lum, P. C. Shor, and H. F. M. Van der Loos, "Development of robots for rehabilitation therapy: The Palo Alto VA/Stanford experience," *J. Rehabil. Res. Develop.*, vol. 37, no. 6, p. 663, 2000.
- [13] R. Loureiro, F. Amirabdollahian, M. Topping, B. Driessen, and W. Harwin, "Upper limb robot mediated stroke therapy—GENTLE/s approach," *Auton. Robots*, vol. 15, no. 1, pp. 35–51, 2003.
- [14] S. Xie, "Advanced robotics for medical rehabilitation: Current state of the art and recent advances," in *Proc. SIGSPATIAL ACM GIS Int. Workshop Secur. Privacy GIS LBS*, 2016.
- [15] J. B. Nielsen, J.-S. Brittain, D. M. Halliday, V. Marchand-Pauvert, D. Mazevet, and B. A. Conway, "Reduction of common motoneuronal drive on the affected side during walking in hemiplegic stroke patients," *Clin. Neurophysiol.*, vol. 119, no. 12, pp. 2813–2818, 2008.
- [16] L. M. Pain, R. Baker, D. Richardson, and A. M. R. Agur, "Effect of trunk-restraint training on function and compensatory trunk, shoulder and elbow patterns during post-stroke reach: A systematic review," *Disab. Rehabil.*, vol. 37, no. 7, pp. 553–562, 2015.
- [17] Y. X. Zhi, M. Lukasik, M. H. Li, E. Dolatabadi, R. H. Wang, and B. Taati, "Automatic detection of compensation during robotic stroke rehabilitation therapy," *IEEE J. Transl. Eng. Health Med.*, vol. 6, 2017, Art. no. 2100107.
- [18] B. A. Valdés and H. F. M. Van der Loos, "Biofeedback vs. game scores for reducing trunk compensation after stroke: A randomized crossover trial," *Topics Stroke Rehabil.*, vol. 25, pp. 1–18, Feb. 2017.
- [19] C. R. Burton, "A description of the nursing role in stroke rehabilitation," *J. Adv. Nursing*, vol. 32, no. 1, pp. 174–181, 2010.
- [20] M. C. Cirstea and M. F. Levin, "Improvement of arm movement patterns and endpoint control depends on type of feedback during practice in stroke survivors," *Neurorehabil. Neural Repair*, vol. 21, no. 5, pp. 398–411, 2007.
- [21] D. R. Bueno, J. M. Lizano, and L. Montano, "Effect of muscular fatigue on fractal upper limb coordination dynamics and muscle synergies," in *Proc. 37th Annu. Int. Conf. IEEE Eng. Med. Biol. Soc.*, Aug. 2015, pp. 6082–6085.
- [22] S. A. Safavynia, G. Torres-Oviedo, and L. Ting, "Muscle synergies: Implications for clinical evaluation and rehabilitation of movement," *Topics Spinal Cord Injury Rehabil.*, vol. 17, no. 1, p. 16, 2011.
- [23] J. C. Cowlley and D. H. Gates, "Proximal and distal muscle fatigue differentially affect movement coordination," *PLoS ONE*, vol. 12, no. 2, 2017, Art. no. e0172835.
- [24] G. Torres-Oviedo and L. H. Ting, "Muscle synergies characterizing human postural responses," *J. Neurophys.*, vol. 98, no. 4, pp. 2144–2156, Oct. 2007.
- [25] Y. P. Ivanenko, G. Cappellini, N. Dominici, R. E. Poppele, and F. Lacquaniti, "Coordination of locomotion with voluntary movements in humans," *J. Neurosci.*, vol. 25, no. 31, pp. 7238–7253, 2005.
- [26] V. C. K. Cheung, L. Piron, M. Agostini, S. Silvoni, A. Turolla, and E. Bizzi, "Stability of muscle synergies for voluntary actions after cortical stroke in humans," *Proc. Nat. Acad. Sci. USA*, vol. 106, no. 46, pp. 19563–19568, Nov. 2009.
- [27] L. Larsson, G. Grimby, and J. Karlsson, "Muscle strength and speed of movement in relation to age and muscle morphology," *J. Appl. Physiol. Respiratory Environ. Exerc. Physiol.*, vol. 46, no. 3, pp. 451–456, 1979.
- [28] S. Pak and C. Patten, "Strengthening to promote functional recovery poststroke: An evidence-based review," *Topics Stroke Rehabil.*, vol. 15, no. 3, pp. 177–199, 2008.
- [29] T. Kostka, "Resistance (strength) training in health promotion and rehabilitation," *Polski Merkuriusz Lekarski Organ Polskiego Towarzystwa Lekarskiego*, vol. 13, no. 78, pp. 520–523, 2002.
- [30] E. Kilic, "EMG based neural network and admittance control of an active wrist orthosis," *J. Mech. Sci. Technol.*, vol. 31, no. 12, pp. 6093–6106, 2017.
- [31] C. Foster, L. L. Hector, R. Welsh, M. Schrage, M. A. Green, and A. C. Snyder, "Effects of specific versus cross-training on running performance," *Eur. J. Appl. Physiol. Occupat. Physiol.*, vol. 70, no. 4, pp. 367–372, Jul. 1995.
- [32] H. Liu, Y. Cao, X. Xie, and Y. Hu, "Estimation of muscle fatigue degree using time-varying autoregressive model parameter estimation of surface electromyography," *Chin. J. Biomed. Eng.*, vol. 26, pp. 493–497, 2007.
- [33] M. Cifrek, V. Medved, S. Tonković, and S. Ostojić, "Surface EMG based muscle fatigue evaluation in biomechanics," *Clin. Biomech.*, vol. 24, no. 4, pp. 327–340, 2009.
- [34] D. Turner, A. Ramos-Murguialday, N. Birbaumer, U. Hoffmann, and A. Luft, "Neurophysiology of robot-mediated training and therapy: A perspective for future use in clinical populations," (in English), *Frontiers Neurol.*, vol. 4, p. 184, Nov. 2013.
- [35] J. P. A. Dewald and R. F. Beer, "Abnormal joint torque patterns in the paretic upper limb of subjects with hemiparesis," *Muscle Nerve*, vol. 24, no. 2, pp. 273–283, Feb. 2001.

- [36] R. Merletti, H. Hermens, and R. Kedefors, "European community projects on surface electromyography," in *Proc. 23rd Annu. Int. Conf. IEEE Eng. Med. Biol. Soc.*, Oct. 2001, pp. 1119–1122.
- [37] M. Mugnosso, F. Marini, M. Holmes, P. Morasso, and J. Zenzeri, "Muscle fatigue assessment during robot-mediated movements," *J. Neuroeng. Rehabil.*, vol. 15, no. 1, p. 119, 2018.
- [38] M. Mugnosso, F. Marini, M. Gillardo, P. Morasso, and J. Zenzeri, "A novel method for muscle fatigue assessment during robot-based tracking tasks," in *Proc. Int. Conf. Rehabil. Robot.*, Jul. 2017, pp. 84–89.
- [39] A. A. Faisal, L. P. J. Selen, and D. M. Wolpert, "Noise in the nervous system," *Nature Rev. Neurosci.*, vol. 9, no. 4, pp. 292–303, 2008.
- [40] A. Roby-Brami, A. Feydy, M. Combeaud, E. V. Biryukova, B. Bussel, and M. F. Levin, "Motor compensation and recovery for reaching in stroke patients," *Acta Neurolog. Scandinavica*, vol. 107, no. 5, pp. 369–381, 2010.
- [41] B. Taati, R. Wang, R. Huq, J. Snoek, and A. Mihailidis, "Vision-based posture assessment to detect and categorize compensation during robotic rehabilitation therapy," in *Proc. 4th IEEE RAS EMBS Int. Conf. Biomed. Robot. Biomechatron.*, Jun. 2012, pp. 1607–1613.
- [42] K. K. A. Bakhti, I. Laffont, M. Muthalib, J. Froger, and D. Mottet, "Kinect-based assessment of proximal arm non-use after a stroke," *J. Neuroeng. Rehabil.*, vol. 15, no. 1, p. 104, Nov. 14 2018.
- [43] M. Vukelić, R. Bauer, G. Naros, I. Naros, C. Braun, and A. Gharabaghi, "Lateralized alpha-band cortical networks regulate volitional modulation of beta-band sensorimotor oscillations," *NeuroImage*, vol. 87, pp. 147–153, Feb. 2014.



**GUOFENG LI** received the B.E. degree in mechatronic engineering from the South China University of Technology, Guangzhou, China, in 2018, where he is currently a Research Student with the Shien-Ming Wu School of Intelligent Engineering. His current research interest includes upper-limb rehabilitation robot design.



**YAN CHEN** received the B.E. degree and M.S. degree in mechatronic engineering from the Hefei University of Technology, Hefei, China, in 2018. He is currently pursuing the Ph.D. degree with the Shien-Ming Wu School of Intelligent Engineering, South China University of Technology, Guangzhou. His research interests include signal processing, machine learning, and upper-limb rehabilitation robotics.

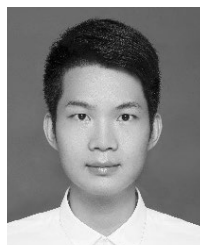


**KE MA** received the B.E. degree in mechanical design manufacture and automation from the Nanjing University of Science and Technology, Nanjing, China, in 2017. He is currently a Research Student with the School of Mechanical and Automotive Engineering, South China University of Technology, Guangzhou. His research interests include analysis and processing of surface electromyography signals.



**LONGHAN XIE** received the B.S. and M.S. degrees in mechanical engineering from Zhejiang University, in 2002 and 2005, respectively, and the Ph.D. degree in mechanical and automation engineering from The Chinese University of Hong Kong, in 2010.

From 2010 to 2016, he was an Assistant Professor and an Associate Professor with the School of Mechanical and Automotive Engineering, South China University of Technology, where he has been a Professor with the Shien-Ming Wu School of Intelligent Engineering, since 2017. His research interests include biomedical engineering and robotics. He is also a member of ASME.



**SHUANGYUAN HUANG** received the B.E. degree in mechatronic engineering from Shandong University, Jinan, China, in 2016. He is currently pursuing the Ph.D. degree with the Shien-Ming Wu School of Intelligent Engineering, South China University of Technology, Guangzhou. His research interests include upper-limb rehabilitation robotics and human-robot interaction.



**SIQI CAI** received the B.E. degree in mechanical engineering from the South China University of Technology, Guangzhou, China, in 2016, where she is currently pursuing the Ph.D. degree with the Shien-Ming Wu School of Intelligent Engineering. Her research interests include biomechanical engineering, upper-limb rehabilitation robotics, and machine learning.

...